nature reviews earth & environment

https://doi.org/10.1038/s43017-023-00427-8

Perspective

Check for updates

Anthropogenic impacts on twentieth-century ENSO variability changes

In the format provided by the authors and unedited

Supplementary Information

for

Anthropogenic impacts on 20th century ENSO variability changes

Wenju Cai[1,2†], Benjamin Ng[2], Tao Geng[1,3], Fan Jia[4], Lixin Wu[1,3†], Guojian Wang[1,2], Yu Liu[5], Bolan Gan[1,3], Kai Yang[6], Agus Santoso[2,7], Xiaopei Lin[1,3], Ziguang Li[1,3], Yi Liu[1], Yun Yang[8], Fei-Fei Jin[9], Mat Collins[10] and Michael J. McPhaden[11]

[1]Frontier Science Center for Deep Ocean Multispheres and Earth System and Key Laboratory of Physical Oceanography, Ocean University of China, Qingdao, China.

[2]Center for Southern Hemisphere Oceans Research (CSHOR), CSIRO Oceans and Atmosphere, Hobart, TAS, Australia.

[3]Laoshan Laboratory, Qingdao, China.

[4]Key Laboratory of Ocean Circulation and Waves, Institute of Oceanology, Chinese Academy of Sciences, Qingdao, China.

[5]The State Key Laboratory of Loess and Quaternary Geology, Institute of Earth Environment, Chinese Academy of Sciences, Xi'an, China.

[6]State Key Laboratory of Numerical Modeling for Atmospheric Sciences and Geophysical Fluid Dynamics, Institute of Atmospheric Physics, Chinese Academy of Sciences, Beijing, China.

[7]Australian Research Council (ARC) Center of Excellence for Climate Extremes, University of New South Wales, Sydney, NSW, Australia.

[8]College of Global Change and Earth System Science, Beijing Normal University, Beijing China.

[9]Department of Atmospheric Science, SOEST, University of Hawaii at Manoa, Honolulu, Hawaii, USA.

[10]Department of Mathematics and Statistics, University of Exeter, Exeter, UK

[11]NOAA/Pacific Marine Environmental Laboratory, Seattle, WA, USA.

[†]email: Wenju Cai (Wenju.cai@csiro.au), Lixin Wu (Lxwu@ouc.edu.cn).

SST reanalysis products and empirical orthogonal function (EOF) analysis. We use six reanalysis products to compare ENSO variability between the pre- and post-1960 periods. These are:

- 20CRv2c multi-member ensemble average of surface temperatures over the ocean (Twentieth Century reanalysis version 2c from 1901 to 2011 (REF.[1]);
- CERA-20C (ECMWF CERA-20C from 1901 to 2010 (REF.[2]);
- ERA-20C sea surface temperatures (ECMWF ERA-20C from 1901 to 2010 (REF.[3]);
- ERSST v3b (Extended Reconstructed SST version 3b from 1901 to 2019 (REF.[4]); and
- HadISST v1.1 (Hadley Centre Sea Ice and SST data set version 1.1 from 1901 to 2020 (REF.[5]).
- COBE Sea Surface Temperature from 1901 to 2020 (REF.[6])

The E-index and C-index from each product are averaged first before analysis to generate multi-product ensemble results presented in Fig. 1. Two analyses are used to examine linear trends of upper oceanic temperatures along the equatorial Pacific, which is presented in Fig. 5b. These are:

- ORA-s3 (ECMWF Ocean Analysis System: ORA-s3 from 1959 to 2011 (REF.[7])
- ORA-s4 (ECMWF Ocean Analysis System: ORA-s4 from 1958 to 2017 (REF.[8]).

We use a traditional fixed location ENSO index (Niño3.4) and indices that separate EP- from CP-ENSO for which, apply EOF analysis to quadratically detrended monthly SST anomalies in an equatorial domain (15°S-15°N, 140°E-80°W). The two dominant modes, each with a principal pattern and a principal component (PC), are combined to describe the two El Niño regimes. Evolution of CP-El Niño and EP-El Niño regimes are described by a C-index ($(PC1+PC2)/\sqrt{2}$) and E-index ($(PC1-PC2)/\sqrt{2}$), respectively.

One experiment each model. We examine 43 CMIP6 models forced with observed historical emissions of greenhouse gases to 2014 and various Shared Socioeconomic Pathways (SSP) 126, 245, 370, and 585. For the 2015-2020 period, we concatenate the historical to the SSP585 simulations but concatenating to other SSP scenarios makes little difference to ENSO variability over the 1961-2020 period. To examine possible ENSO changes, we use traditional Niño3.4 index, as well as E-index and C-index. SST anomalies with reference to the monthly climatology of 1901-2020 are detrended and concatenated to depict ENSO evolution over the

full period spanning from piControl to 2100.

We apply EOF analysis to monthly SST anomalies in each model over the period 1901-2020, such that in each model, the C-index and E-index have a standard deviation of one over the 120 years so that they are comparable across models. ENSO indices over the rest of the full period are obtained by projecting onto the EOF patterns in a subset of 39 models that have at least 300 years of piControl. The EOF analysis generates 39 virtual worlds each covering from a multi-century preindustrial period to 2020. Likewise, conventional ENSO indices over the full period are constructed and scaled by the standard deviation over the 1901-2020 period.

Large ensemble experiments. In the 'model democracy' (that is, one experiment each model) approach, the distinction between uncertainties from internal variability and from model structure is not clear. One way to isolate the impact of internal variability is to create an ensemble of simulations with a single climate model, by applying an infinitesimal perturbation to the initial condition of each member of experiments. Due to butterfly effect, the perturbation creates diverging weather and climate trajectories including ENSO, inducing an ensemble spread. Because the resulting sequences of internal variability are randomly phased and independent among the individual experiment, the forced change resulting from the common climate change forcing is examined qualitatively by assessing whether a majority of experiments produce a consistent change, and quantitatively by averaging over the experiments.

We use all available CMIP6 large ensemble experiments in models with at least 10 experiments initiated from a time before 1900 (Supplementary Table 1). Each model is forced by the same historical anthropogenic and natural forcings from 1850 to 2014 and from 2015 to 2020 under one or more emission scenarios (SSP126, SSP245, SSP370 and SSP585). In the 2015-2020 period, the difference in projected radiative forcing among emission scenarios is small, and we choose a scenario from each model that has the largest number of experiments. In total, there are seven models with a total of 282 experiments. We compare amplitude of ENSO variability between the pre- and post-1960 period.

Pre-industrial multi-century-long experiments. Another approach to assess impact of transient greenhouse warming involves comparing ENSO variability in a period (60-year) with a probability distribution in a baseline period without or with little influence from greenhouse warming, referred to as 'noise'. Diagnosis of noise is performed using multi-century-long piControl experiments without climate change. The noise is compared to a potential signal

using a ‘signal-to-noise’ ratio threshold. A ratio greater than 2.0 indicates that the signal is greater than the 95 percentile of the noise, that is, unusually strong sitting within the top 5% value of the baseline distribution.

Outputs from 39 climate models participating in CMIP6 in the ‘model democracy’ approach are used to evaluate how unusual the observed post-1960 ENSO is, compared to the range of fluctuations due to internal variability without greenhouse warming in long piControl simulation of at least 300 years (Supplementary Table 2). These model outputs are concatenated to a historical simulation starting from the mid-19th century and forced with historical forcings to 2014, and a future warming experiment from 2015 under SSP585, sharing a common integration period of 1850-2100.

Statistical significance test. A Bootstrap method[10] is used to examine whether the increased ENSO variability in the post-1960 is statistically significant. Although the multi-model average largely removes the influence from internal variability, there is still some residual influence from internal variability. To gauge the size of the residual influence, the 43 values of the ENSO index variability in Fig. 2a in the pre-1960 period from the 43 models are re-sampled randomly to construct 10,000 realisations of mean variability. In this random re-sampling process, a sample is allowed to be selected again. The standard deviation of the 10,000 inter-realisations of mean variability in the pre-1960 is determined. The same is carried out for the post-1960 period. The increased variability of ENSO index in the future period is greater than the sum of the two re-sampling standard deviation values, indicating that the variability difference between the two periods is statistical significance above the 95% confidence level (Fig. 2a & Fig. 2b). Identical analysis is carried out for the multi-member experiments (Fig. 3b & Fig. 3d).

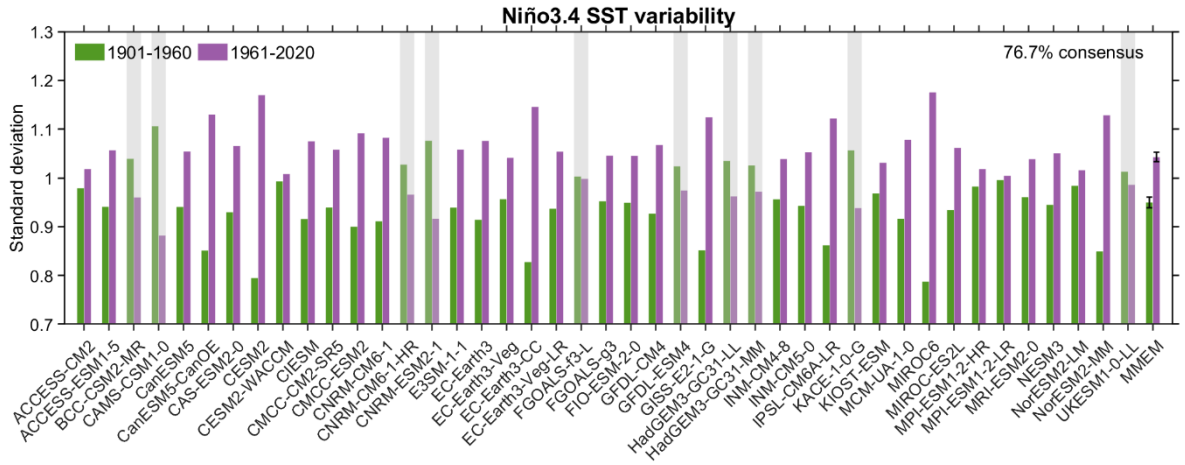

Supplementary Fig. 1 | Inter-model consensus on increased ENSO SST variability after 1960. ENSO Niño3.4 SST standard deviation for the 1901-1960 and 1961-2020 periods from 43 available CMIP6 models. The green and purple bars represent the 1901-1960 and 1961-2020 periods, respectively. The grey shading indicates models which do not simulate an increase in ENSO standard deviation. Majority (76.7%) of models simulate an increase in ENSO Niño SST variability. Error bars on the multi-model mean are calculated as 1.0 standard deviation of 10,000 inter-realisations of a Bootstrap method.

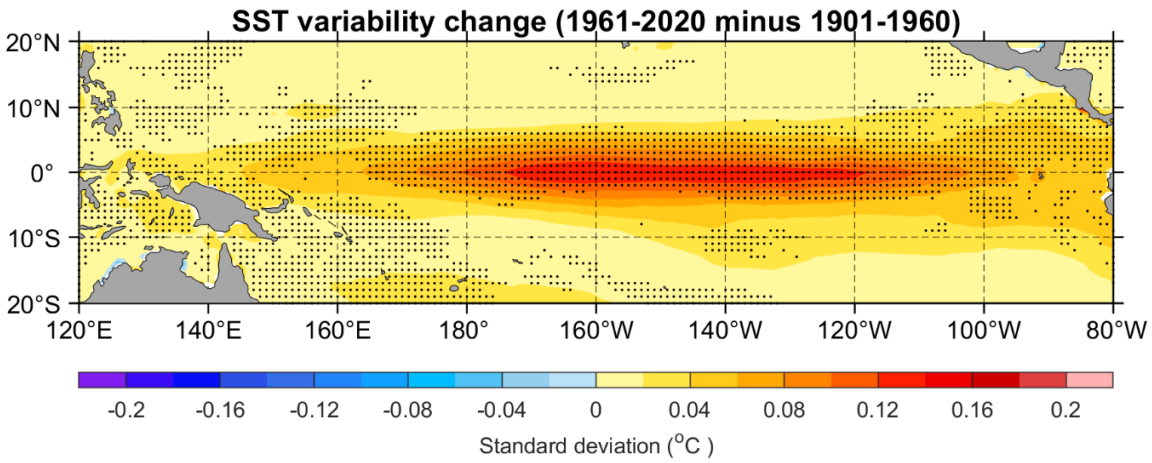

Supplementary Fig. 2 | Inter-model consensus on increased ENSO grid-point SST variability after 1960. Multi-model mean change of grid-point SST standard deviation (°C) between 1901-1960 and 1961-2020. Stippling indicates that more than 70% of models show a same-signed change.

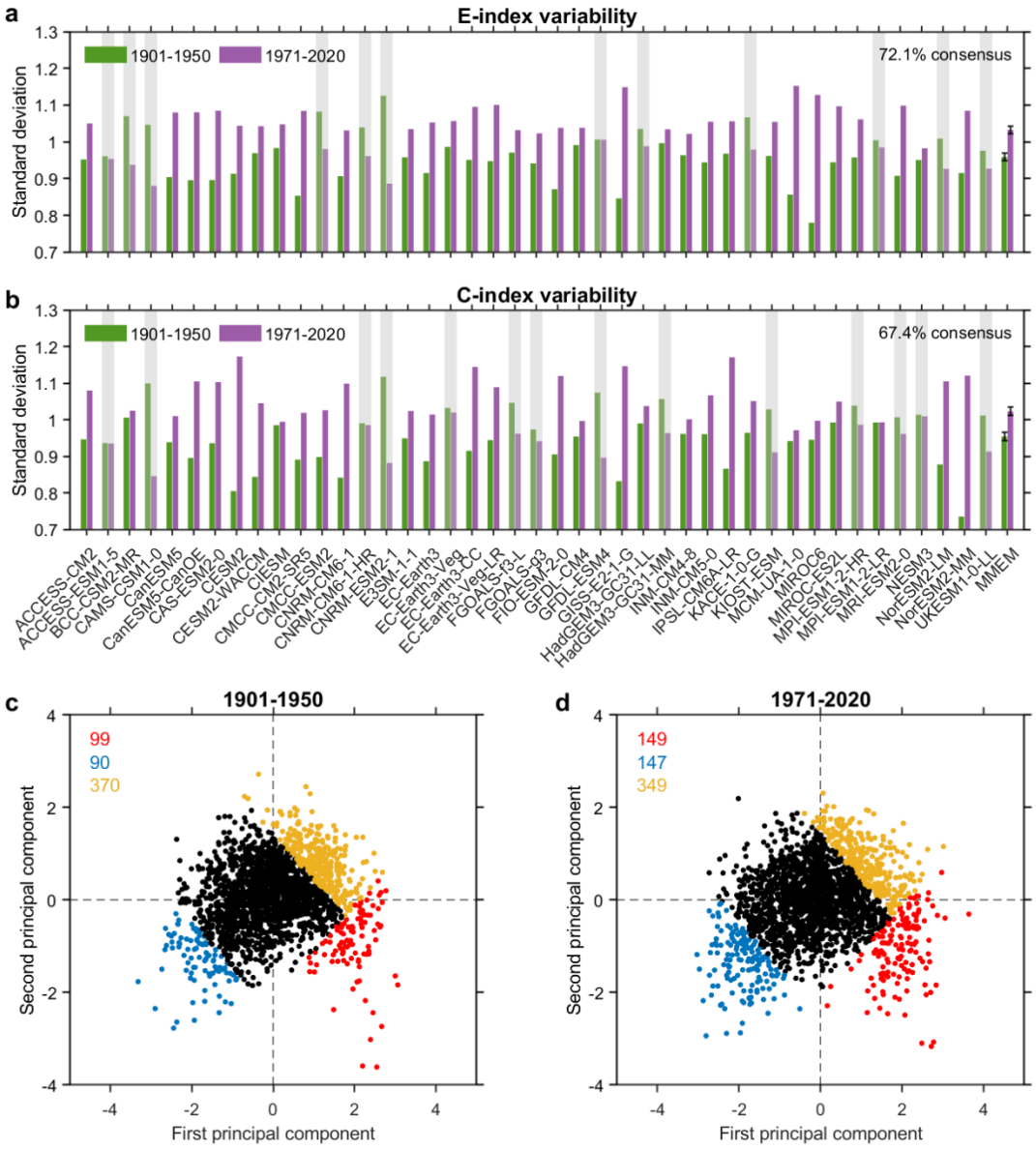

Supplementary Fig. 3 | Simulated increase in post-1970 ENSO variability. (a, b) | E-index and C-index standard deviation (s.d.) for the 1901-1950 and 1971-2020 periods from 43 available CMIP6 models. The green and purple bars represent the 1901-1950 and 1971-2020 periods, respectively. The grey shading indicates models which do not simulate an increase in ENSO variability. The percentage of models that simulate an increase is denoted on the top right. The range in the multi-model mean bars is defined as the two s.d. value of inter-model variability. **(c, d)** | Nonlinear relationship between the first and second principal components for the 1901 to 1960 period, and the 1971 to 2020 period, respectively. The blue, orange, and red dots indicate strong La Niña, central Pacific El Niño, and strong eastern Pacific El Niño events, respectively. The coloured numbers indicate the frequency of each type of events.

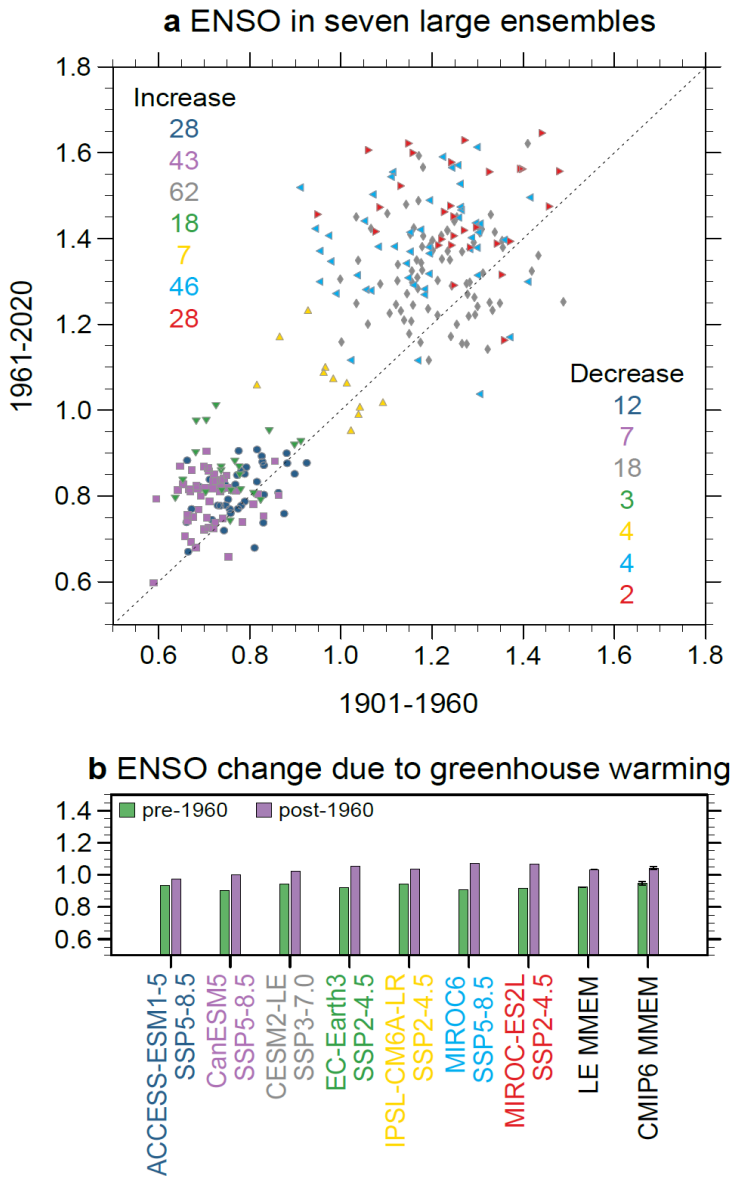

Supplementary Fig. 4 | Increased post-1960 Niño3.4 variability in butterfly-effect ensembles of experiments. **a** | Pre-1960 (1901-1960) variability versus post-1960 (1961-2020) variability for seven large ensembles in seven models. Number of experiments in each model producing an increase (decrease) in post-1960 ENSO variability is indicated in the top-left (bottom right) corner. Different SSPs are chosen to concatenate time series for the period of 2015-2020 because the SSP has the largest number of experiments (see Supplementary Table 1). **b** | Large ensemble mean Niño3.4 variability in the pre-1960 and the post-1960 60-year periods. The Niño3.4 index for each ensemble experiment is standardised over the full 1901-2020 period before calculating the ensemble average. The mean across the seven large ensemble averages is shown in the 2nd group of bars from right (LE MMEM) and the CMIP6 MMEM of the model democracy approach is also shown. The error bars represent the ±1.0 standard deviation range using a Bootstrap method.

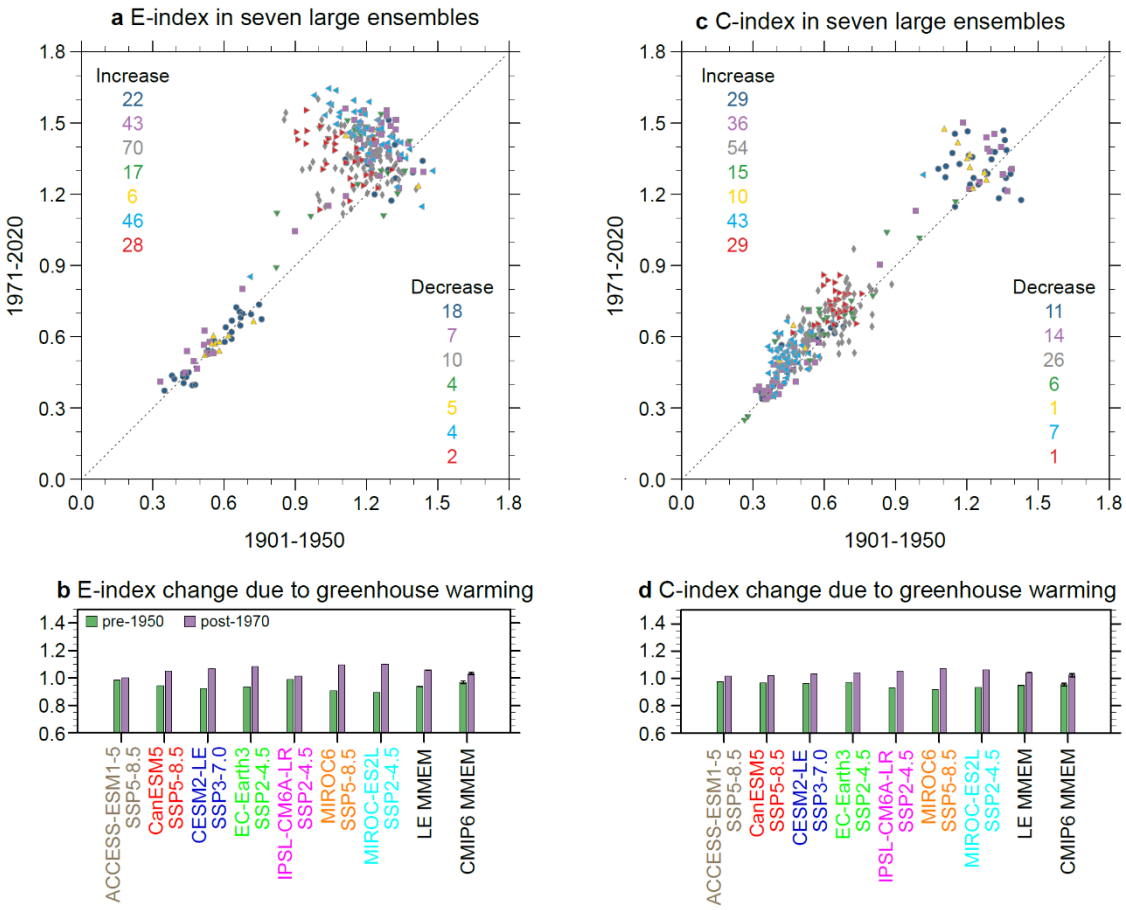

Supplementary Fig. 5 | Increased post-1960 ENSO variability in butterfly-effect ensembles of experiments. **a** | Pre-1950 (1901-1950) variability versus post-1970 (1971-2020) E-index variability for large ensembles in seven models. Number of experiments in each model producing an increase (decrease) in post-1970 ENSO variability is indicated in the top-left (bottom right) corner. Different SSPs are chosen to concatenate time series for the period of 2015-2020 to allow the largest number of experiments (Supplementary Table 1). **b** | Large ensemble mean E-index variability in the pre-1960 and the post-1960 60-year periods. The E-index for each ensemble experiment is standardised over the 1901-2020 period before calculating the ensemble average. The mean across the seven large ensemble averages is shown in the 2nd group of bars from right (LE MMEM) and the CMIP6 MMEM of the model democracy approach is also shown. The error bars represent the ±1.0 standard deviation range using a Bootstrap method. (**c, d**) | The same as (**a, b**), respectively, but for C-index.

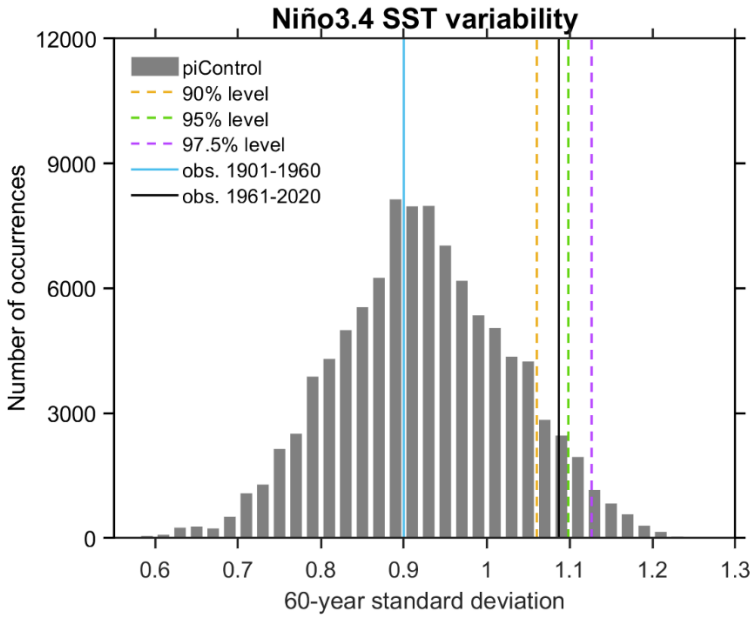

Supplementary Fig. 6 | High variability of the post-1960 ENSO. Histogram (grey bars) of 100,000 realisations of a Bootstrap method for 60-year running standard deviation (s.d.) of Niño3.4 SST in piControl from all 39 CMIP6 models that have at least 300 years of piControl. The dashed yellow, green and purple lines indicate the upper 10, 5 and 2.5 percentile values of the histogram. Observed Niño3.4 SST variability (s.d.) in 1901-1960 and 1961-2020, averaged from multiple reanalysis datasets, are shown in solid blue and black lines, respectively. All the indices are normalised with reference to the 1901-2020 period prior to analysis.

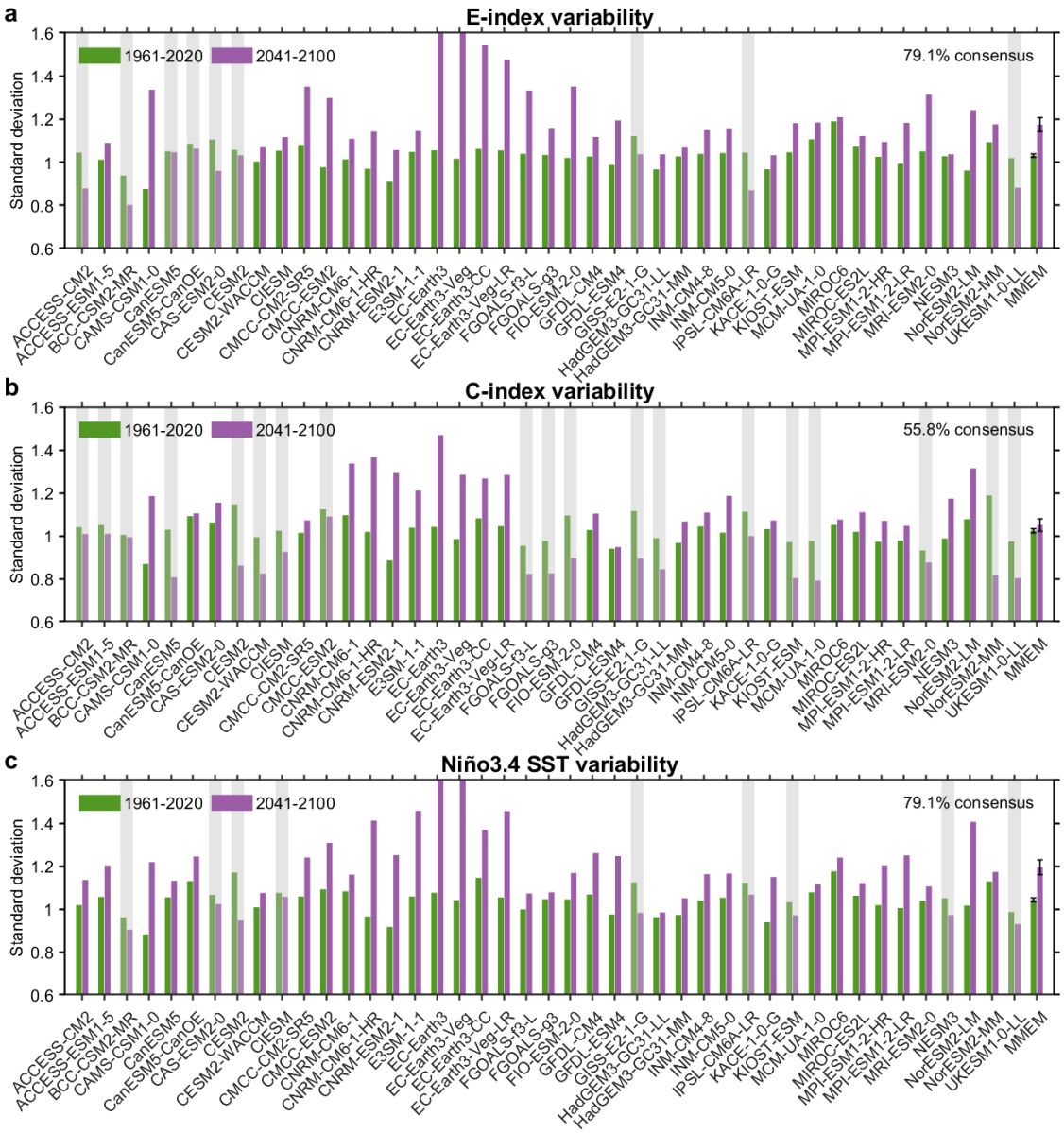

Supplementary Fig. 7 | Projected increase in future ENSO variability. a | E-index standard deviation for the 1961-2020 (green bars) and 2041-2100 (purple bars) periods from 43 available CMIP6 models. Models that simulate a decrease are greyed out. Error bars on the multi-model mean are calculated as 1.0 standard deviation of 10,000 inter-realisations of a Bootstrap method. The percentage of models that simulate an increase is also denoted on the top right. (**b**, **c**) | Same as **a**, respectively, but for (**b**) C-index, (**c**) Niño3.4 index. All the indices are normalised with reference to the 1901-2020 period prior to analysis.

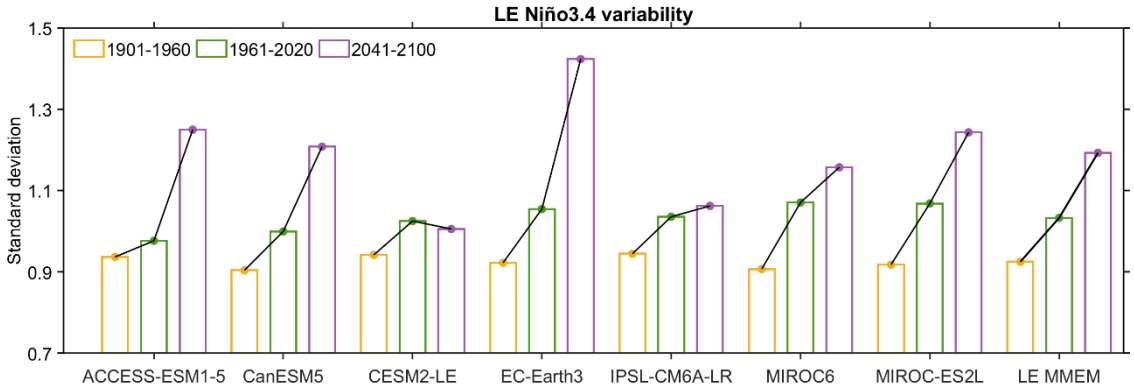

Supplementary Fig. 8 | Continued increase of ENSO variability into the future. Multi-experiment mean Niño3.4 standard deviation for the 1901-1960 (yellow-edge bars), 1961-2020 (green-edge bars) and 2041-2100 (purple-edge bars) periods from each butterfly-effect large ensemble (LE) experiments and the multi-model ensemble average (MMEM). ENSO variability progressively increases into the future in majority of models.

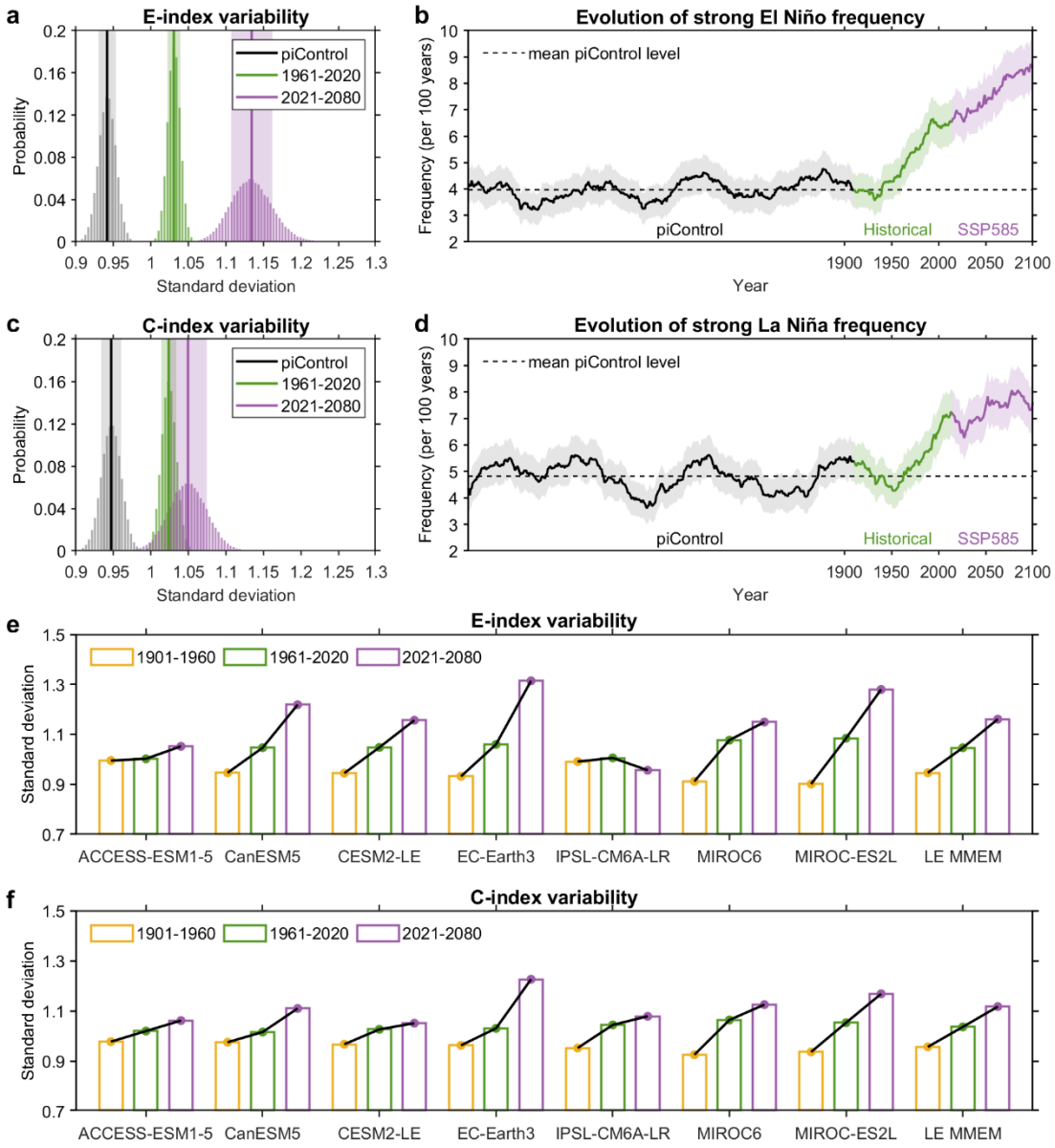

Supplementary Fig. 9 | Continued increase of ENSO variability into the future period of 2021-2080. (**a**) | Histogram of 100, 000 realisations of 39-value ensemble means of a Bootstrap method on 60-year running standard deviation of E-index in piControl (gray bars), E-index standard deviation in the 1961-2020 (green bars) and the 2021-2080 (purple bars) periods, respectively, from the 39 CMIP6 models that have at least 300 years of piControl. Solid lines and shadings indicate multi-model mean and 1.0 s.d. of the 100,000 inter-realisations respectively. (**b**) | Evolution of strong El Niño frequency (events per 100 years) simulated over a period from piControl to 2100, diagnosed in 60-year sliding windows moving forward from the start of the last 300 years of piControl (black), covering the entire historical period till 2014 (green) and extending into the 21st century under a high-emission scenario SSP585 (purple). Solid lines and shadings indicate multi-model mean and 95% confidence intervals based on a

Poisson distribution, respectively. The dashed black line indicates the mean level of piControl. (**c**, **d**) | Same as (**a, b**) but for C-index variability and strong La Niña frequency, respectively. (**e, f**) | Multi-experiment mean E-index and C-index standard deviation for the 1901-1960 (yellow-edge bars), 1961-2020 (green-edge bars) and 2021-2080 (purple-edge bars) periods from each butterfly effect large ensemble (LE) experiments and the multi-model ensemble average (MMEM). ENSO variability progressively increases into the future, featuring an increasing frequency of strong El Niño and strong La Niña events.

Supplementary Table 1 | Information of CMIP6 butterfly-effect large ensemble of experiments used in this study. Names of models, the associated institutions and countries, number of experiments, and emission scenarios used in this study.

Model	Institute, Country	Number of experiments	SSP used
ACCESS-ESM1-5[11,12]	CSIRO, Australia	40	SSP585
CanESM5[13,14]	CCCMA, Canada	50	SSP585
CESM2-LE[15]	NCAR, USA; ICCP, Korea	80	SSP370
EC-Earth3[16,17]	Europe-wide consortium	21	SSP245
IPSL-CM6A-LR[18,19]	IPSL, France	11	SSP245
MIROC6[20,21]	JAMSTEC, Japan	50	SSP585
MIROC-ES2L[22,23]	JAMSTEC, Japan	30	SSP245

Supplementary Table 2 | Information of CMIP6 models used in this study. Names of models, the associated institutions and countries, their ensemble members, length of piControl experiemnt, and emission scenarios used in this study.

Model	Institute, Country	Ensemble	piControl years	SSP used
ACCESS-CM2[24,25]	CSIRO, Australia	r1i1p1f1	500	SSP585
ACCESS-ESM1-5[11,12]	CSIRO, Australia	r1i1p1f1	1000	SSP585
BCC-CSM2-MR[26,27]	BCC, China	r1i1p1f1	600	SSP585
CAMS-CSM1-0[28,29]	CAMS, China	r1i1p1f1	500	SSP585
CAS-ESM2-0[30,31]	CAS, China	r1i1p1f1	549	SSP585
CESM2[32,33]	NCAR, USA	r4i1p1f1	NAN	SSP585
CESM2-WACCM[34,35]	NCAR, USA	r1i1p1f1	499	SSP585
CIESM[36,37]	Tsinghua University, China	r1i1p1f1	500	SSP585
CMCC-CM2-SR5[38,39]	CMCC, Italy	r1i1p1f1	500	SSP585
CMCC-ESM2[40,41]	CMCC, Italy	r1i1p1f1	500	SSP585
CNRM-CM6-1[42,43]	CNRM, France	r1i1p1f2	500	SSP585
CNRM-CM6-1-HR[44,45]	CNRM, France	r1i1p1f2	300	SSP585
CNRM-ESM2-1[46,47]	CNRM, France	r1i1p1f2	500	SSP585
CanESM5[13,14]	CCCMA, Canada	r1i1p1f1	1000	SSP585
CanESM5-CanOE[48,49]	CCCMA, Canada	r1i1p2f1	501	SSP585
E3SM-1-1[50,51]	DOE, USA	r1i1p1f1	251	SSP585
EC-Earth3[16,52]	Europe-wide consortium	r1i1p1f1	459	SSP585
EC-Earth3-CC[53,54]	Europe-wide consortium	r1i1p1f1	505	SSP585
EC-Earth3-Veg[55,56]	Europe-wide consortium	r1i1p1f1	500	SSP585
EC-Earth3-Veg-LR[57,58]	Europe-wide consortium	r1i1p1f1	501	SSP585
FGOALS-f3-L[59,60]	CAS, China	r1i1p1f1	500	SSP585
FGOALS-g3[61,62]	CAS, China	r1i1p1f1	700	SSP585
FIO-ESM-2-0[63,64]	FIO, China	r1i1p1f1	575	SSP585
GFDL-CM4[65,66]	NOAA-GFDL, USA	r1i1p1f1	500	SSP585
GFDL-ESM4[67,68]	NOAA-GFDL, USA	r1i1p1f1	500	SSP585
GISS-E2-1-G[69,70]	NASA/GISS, USA	r1i1p1f2	345	SSP585
HadGEM3-GC31-LL[71,72]	MOHC, UK	r1i1p1f3	2000	SSP585
HadGEM3-GC31-MM[73,74]	MOHC, UK	r1i1p1f3	500	SSP585
INM-CM4-8[75,76]	INM, Russia	r1i1p1f1	531	SSP585
INM-CM5-0[77,78]	INM, Russia	r1i1p1f1	1201	SSP585
IPSL-CM6A-LR[18,79]	IPSL, France	r1i1p1f1	2000	SSP585
KACE-1-0-G[80,81]	NIMS-KMA, Korea	r1i1p1f1	NAN	SSP585
KIOST-ESM[82,83]	KIOST, Korea	r1i1p1f1	150	SSP585
MCM-UA-1-0[84,85]	UA, USA	r1i1p1f2	500	SSP585
MIROC6[20,21]	JAMSTEC, Japan	r1i1p1f1	800	SSP585
MIROC-ES2L[22,86]	JAMSTEC, Japan	r1i1p1f2	500	SSP585
MPI-ESM1-2-HR[87,88]	MPI-M, Germany	r1i1p1f1	500	SSP585
MPI-ESM1-2-LR[89,90]	MPI-M, Germany	r1i1p1f1	1000	SSP585
MRI-ESM2-0[91,92]	MRI, Japan	r1i1p1f1	701	SSP585

NESM3[93,94]	NUIST, China	r1i1p1f1	500	SSP585
NorESM2-LM[95,96]	NCC, Norway	r1i1p1f1	501	SSP585
NorESM2-MM[97,98]	NCC, Norway	r1i1p1f1	500	SSP585
UKESM1-0-LL[99,100]	MOHC, UK	r1i1p1f2	1000	SSP585

Supplementary References

1. Compo, G. P. *et al.* The twentieth century reanalysis project. *Quarterly Journal of the Royal Meteorological Society* **137**, 1–28 (2011).
2. Laloyaux, P. *et al.* CERA-20C: A coupled reanalysis of the twentieth century. *J. Adv. Model. Earth Syst.* **10**, 1172–1195 (2018).
3. Poli, P. *et al.* ERA-20C: An atmospheric reanalysis of the twentieth century. *J. Clim.* **29**, 4083–4097 (2016).
4. Smith, T. M., Reynolds, R. W., Peterson, T. C. & Lawrimore, J. Improvements to NOAA's historical merged land-ocean surface temperature analysis (1880-2006). *J. Clim.* **21**, 2283–2296 (2008).
5. Rayner, N. A. et al. Global analyses of sea surface temperature, sea ice, and night marine air temperature since the late nineteenth century. *J. Geophys. Res.* **108,** 4407 (2003).
6. Ishii, M., Shouji, A., Sugimoto, S., & Matsumoto, T. Objective Analyses of Sea-Surface Temperature and Marine Meteorological Variables for the 20th Century using ICOADS and the Kobe Collection. *Int. J. Climatol.*, **25**, 865-879 (2005).
7. Balmaseda, M. A., Vidard, A. & Anderson, D. L. T. The ECMWF ocean analysis system: ORA-S3. *Mon. Weath Rev.* **136**, 3018–3034 (2008).
8. Balmaseda, M. A., Mogensen, K. & Weaver, A. T. Evaluation of the ECMWF ocean reanalysis system ORAS4. *Q. J. R. Meteorol. Soc.* **139**, 1132–1161 (2013).
9. Lorenz, E. N. Empirical orthogonal functions and statistical weather prediction. *Statistical Forcast Project Report 1 (MIT Department of Meterology,* 1956).
10. Austin, P. C. & Tu, J. V. Bootstrap methods for developing predictive models. *The American Statistician*. **58**, 131-137 (2004).
11. Ziehn, T. et al. *CSIRO ACCESS-ESM1.5 Model Output Prepared for CMIP6 CMIP Historical* Version 20210201 (Earth System Grid Federation, 2019); https://doi.org/10.22033/ESGF/CMIP6.4272
12. Ziehn, T. et al. *CSIRO ACCESS-ESM1.5 Model Output Prepared for CMIP6 ScenarioMIP ssp585* Version 20210201 (Earth System Grid Federation, 2019); https://doi.org/10.22033/ESGF/CMIP6.4333
13. Swart, N. C. et al. *CCCma CanESM5 Model Output Prepared for CMIP6 CMIP Historical* Version 20210201 (Earth System Grid Federation, 2019); https://doi.org/10.22033/ESGF/CMIP6.3610
14. Swart, N. C. et al. *CCCma CanESM5 Model Output Prepared for CMIP6 ScenarioMIP ssp585* Version 20210201 (Earth System Grid Federation, 2019); https://doi.org/10.22033/ESGF/CMIP6.3696
15. Rodgers, K. B. et al. Ubiquity of human-induced changes in climate variability. *Earth Syst. Dyn.* **12**, 1393-1411 (2021).
16. EC-Earth Consortium (EC-Earth). *EC-Earth-Consortium EC-Earth3 Model Output Prepared for CMIP6 CMIP Historical* Version 20210201 (Earth System Grid Federation, 2019); https://doi.org/10.22033/ESGF/CMIP6.4700
17. EC-Earth Consortium (EC-Earth). *EC-Earth-Consortium EC-Earth3 Model Output Prepared for CMIP6 ScenarioMIP ssp245* Version 20210201 (Earth System Grid Federation, 2019); https://doi.org/10.22033/ESGF/CMIP6.4880
18. Boucher, O. et al. *IPSL IPSL-CM6A-LR Model Output Prepared for CMIP6 CMIP Historical* Version 20210201 (Earth System Grid Federation, 2019); https://doi.org/10.22033/ESGF/CMIP6.5195
19. Boucher, O. et al. *IPSL IPSL-CM6A-LR Model Output Prepared for CMIP6 ScenarioMIP ssp245* Version 20210201 (Earth System Grid Federation, 2019); https://doi.org/10.22033/ESGF/CMIP6.5264
20. Tatebe, H. & Watanabe, M. *MIROC MIROC6 Model Output Prepared for CMIP6 CMIP Historical* Version 20210201 (Earth System Grid Federation, 2019); https://doi.org/10.22033/ESGF/CMIP6.5603
21. Shiogama, H., Abe, M. & Tatebe, H. *MIROC MIROC6 Model Output Prepared for CMIP6 ScenarioMIP ssp585* Version 20210201 (Earth System Grid Federation, 2019); https://doi.org/10.22033/ESGF/CMIP6.5771
22. Hajima, T. et al. *MIROC MIROC-ES2L Model Output Prepared for CMIP6 CMIP Historical* Version 20210201 (Earth System Grid Federation, 2019); https://doi.org/10.22033/ESGF/CMIP6.5602

23. Tachiiri K. et al. *MIROC MIROC-ES2L Model Output Prepared for CMIP6 ScenarioMIP ssp245* Version 20210201 (Earth System Grid Federation, 2019); https://doi.org/10.22033/ESGF/CMIP6.5745
24. Dix, M. et al. *CSIRO-ARCCSS ACCESS-CM2 model output prepared for CMIP6 CMIP Historical* Version 20210201 (Earth System Grid Federation, 2019); https://doi.org/10.22033/ESGF/CMIP6.4271
25. Dix, M. et al. *CSIRO-ARCCSS ACCESS-CM2 model output prepared for CMIP6 ScenarioMIP ssp585* Version 20210201 (Earth System Grid Federation, 2019); https://doi.org/10.22033/ESGF/CMIP6.4332
26. Wu, T. et al. *BCC BCC-CSM2MR Model Output Prepared for CMIP6 CMIP Historical* Version 20210201 (Earth System Grid Federation, 2018); https://doi.org/10.22033/ESGF/CMIP6.2948
27. Xin, X. et al. *BCC BCC-CSM2MR Model Output Prepared for CMIP6 ScenarioMIP ssp585* Version 20210201 (Earth System Grid Federation, 2019); https://doi.org/10.22033/ESGF/CMIP6.3050
28. Rong, X. et al. *CAMS CAMS-CSM1.0 Model Output Prepared for CMIP6 CMIP Historical* Version 20210201 (Earth System Grid Federation, 2019); https://doi.org/10.22033/ESGF/CMIP6.9754
29. Rong, X. et al. *CAMS CAMS-CSM1.0 Model Output Prepared for CMIP6 ScenarioMIP ssp585* Version 20210201 (Earth System Grid Federation, 2019); https://doi.org/10.22033/ESGF/CMIP6.11052
30. Chai, Z. et al. *CAS CAS-ESM1.0 Model Output Prepared for CMIP6 CMIP Historical* Version 20210201 (Earth System Grid Federation, 2020); https://doi.org/10.22033/ESGF/CMIP6.3353
31. Chai, Z. et al. *CAS CAS-ESM1.0 Model Output Prepared for CMIP6 ScenarioMIP ssp585* Version 20201230 (Earth System Grid Federation, 2018).
32. Danabasoglu, G. et al. *NCAR CESM2 Model Output Prepared for CMIP6 CMIP Historical* Version 20210201 (Earth System Grid Federation, 2019); https://doi.org/10.22033/ESGF/CMIP6.7627
33. Danabasoglu, G. et al. *NCAR CESM2 Model Output Prepared for CMIP6 ScenarioMIP ssp585* Version 20210201 (Earth System Grid Federation, 2019); https://doi.org/10.22033/ESGF/CMIP6.7768
34. Danabasoglu, G. et al. *NCAR CESM2-WACCM Model Output Prepared for CMIP6 CMIP Historical* Version 20210201 (Earth System Grid Federation, 2019); https://doi.org/10.22033/ESGF/CMIP6.10071
35. Danabasoglu, G. et al. *NCAR CESM2-WACCM Model Output Prepared for CMIP6 ScenarioMIP ssp585* Version 20210201 (Earth System Grid Federation, 2019); https://doi.org/10.22033/ESGF/CMIP6.10115
36. Huang, W. et al. *THU CIESM Model Output Prepared for CMIP6 CMIP Historical* Version 20210201 (Earth System Grid Federation, 2019); https://doi.org/10.22033/ESGF/CMIP6.8843
37. Huang, W. et al. *THU CIESM Model Output Prepared for CMIP6 ScenarioMIP ssp585* Version 20210201 (Earth System Grid Federation, 2020); https://doi.org/10.22033/ESGF/CMIP6.8863
38. Lovato, T. & Peano, D. *CMCC CMCC-CM2-SR5 Model Output Prepared for CMIP6 CMIP Historical* Version 20210201 (Earth System Grid Federation, 2020); https://doi.org/10.22033/ESGF/CMIP6.3825
39. Lovato, T. & Peano, D. *CMCC CMCC-CM2-SR5 Model Output Prepared for CMIP6 ScenarioMIP ssp585* Version 20210201 (Earth System Grid Federation, 2020); https://doi.org/10.22033/ESGF/CMIP6.3896
40. Lovato, T. et al. *CMCC CMCC-ESM2 Model Output Prepared for CMIP6 CMIP Historical* Version 20210201 (Earth System Grid Federation, 2021); https://doi.org/10.22033/ESGF/CMIP6.13195
41. Lovato, T. et al. *CMCC CMCC-ESM2 Model Output Prepared for CMIP6 ScenarioMIP ssp585* Version 20210201 (Earth System Grid Federation, 2021); https://doi.org/10.22033/ESGF/CMIP6.13259
42. Voldoire, A. *CMIP6 simulations of the CNRM-CERFACS based on CNRM-CM6-1 model for CMIP experiment historical* Version 20210201 (Earth System Grid Federation, 2018); https://doi.org/10.22033/ESGF/CMIP6.4066
43. Voldoire, A. *CNRM-CERFACS CNRM-CM6-1 Model Output Prepared for CMIP6 ScenarioMIP ssp585* Version 20210201 (Earth System Grid Federation, 2019); https://doi.org/10.22033/ESGF/CMIP6.4224
44. Voldoire, A. *CNRM-CERFACS CNRM-CM6-1-HR Model Output Prepared for CMIP6 CMIP Historical* Version 20210201 (Earth System Grid Federation, 2019); https://doi.org/10.22033/ESGF/CMIP6.4067
45. Voldoire, A. *CNRM-CERFACS CNRM-CM6-1-HR Model Output Prepared for CMIP6 ScenarioMIP ssp585* Version 20210201 (Earth System Grid Federation, 2019); https://doi.org/10.22033/ESGF/CMIP6.4225
46. Seferian, R. *CNRM-CERFACS CNRM-ESM2-1 Model Output Prepared for CMIP6 CMIP Historical* Version 20210201 (Earth System Grid Federation, 2018); https://doi.org/10.22033/ESGF/CMIP6.4068

47. Voldoire, A. *CNRM-CERFACS CNRM-ESM2-1 Model Output Prepared for CMIP6 ScenarioMIP ssp585* Version 20210201 (Earth System Grid Federation, 2019); https://doi.org/10.22033/ESGF/CMIP6.4226
48. Swart, N. C. et al. *CCCma CanESM5-CanOE Model Output Prepared for CMIP6 CMIP Historical* Version 20210201 (Earth System Grid Federation, 2019); https://doi.org/10.22033/ESGF/CMIP6.10260
49. Swart, N. C. et al. *CCCma CanESM5-CanOE Model Output Prepared for CMIP6 ScenarioMIP ssp585* Version 20210201 (Earth System Grid Federation, 2019); https://doi.org/10.22033/ESGF/CMIP6.10276
50. Bader, D. C., Leung, R., Taylor, M. & McCoy, R. B. *E3SM-Project E3SM1.1 Model Output Prepared for CMIP6 CMIP Historical* Version 20210201 (Earth System Grid Federation, 2019); https://doi.org/10.22033/ESGF/CMIP6.11485
51. Bader, D. C., Leung, R., Taylor, M. & McCoy, R. B. *E3SM-Project E3SM1.1 Model Output Prepared for CMIP6 ScenarioMIP ssp585* Version 20210201 (Earth System Grid Federation, 2020); https://doi.org/10.22033/ESGF/CMIP6.15179
52. EC-Earth Consortium (EC-Earth). *EC-Earth-Consortium EC-Earth3 Model Output Prepared for CMIP6 ScenarioMIP ssp585* Version 20210201 (Earth System Grid Federation, 2019); https://doi.org/10.22033/ESGF/CMIP6.4912
53. EC-Earth Consortium (EC-Earth). *EC-Earth-Consortium EC-Earth-3-CC Model Output Prepared for CMIP6 CMIP Historical* Version 20210201 (Earth System Grid Federation, 2021); https://doi.org/10.22033/ESGF/CMIP6.4702
54. EC-Earth Consortium (EC-Earth). *EC-Earth-Consortium EC-Earth3-CC Model Output Prepared for CMIP6 ScenarioMIP ssp585* Version 20210201 (Earth System Grid Federation, 2021); https://doi.org/10.22033/ESGF/CMIP6.15636
55. EC-Earth Consortium (EC-Earth). *EC-Earth-Consortium EC-Earth3-Veg Model Output Prepared for CMIP6 CMIP Historical* Version 20210201 (Earth System Grid Federation, 2019); https://doi.org/10.22033/ESGF/CMIP6.4706
56. EC-Earth Consortium (EC-Earth). *EC-Earth-Consortium EC-Earth3-Veg Model Output Prepared for CMIP6 ScenarioMIP ssp585* Version 20210201 (Earth System Grid Federation, 2019); https://doi.org/10.22033/ESGF/CMIP6.4914
57. EC-Earth Consortium (EC-Earth). *EC-Earth-Consortium EC-Earth3-Veg-LR Model Output Prepared for CMIP6 CMIP Historical* Version 20210201 (Earth System Grid Federation, 2020); https://doi.org/10.22033/ESGF/CMIP6.4707
58. EC-Earth Consortium (EC-Earth). *EC-Earth-Consortium EC-Earth3-Veg-LR Model Output Prepared for CMIP6 ScenarioMIP ssp585* Version 20210201 (Earth System Grid Federation, 2020); https://doi.org/10.22033/ESGF/CMIP6.4915
59. Yu, Y. *CAS FGOALS-f3-L Model Output Prepared for CMIP6 CMIP Historical* Version 20210201 (Earth System Grid Federation, 2019); https://doi.org/10.22033/ESGF/CMIP6.3355
60. Yu, Y. *CAS FGOALS-f3-L Model Output Prepared for CMIP6 ScenarioMIP ssp585* Version 20210201 (Earth System Grid Federation, 2019); https://doi.org/10.22033/ESGF/CMIP6.3502
61. Li, L. *CAS FGOALS-g3 Model Output Prepared for CMIP6 CMIP Historical* Version 20210201 (Earth System Grid Federation, 2019); https://doi.org/10.22033/ESGF/CMIP6.3356
62. Li, L. *CAS FGOALS-g3 Model Output Prepared for CMIP6 ScenarioMIP ssp585* Version 20210201 (Earth System Grid Federation, 2019); https://doi.org/10.22033/ESGF/CMIP6.3503
63. Song, Z. et al. *FIO-QLNM FIO-ESM2.0 Model Output Prepared for CMIP6 CMIP Historical* Version 20210201 (Earth System Grid Federation, 2019); https://doi.org/10.22033/ESGF/CMIP6.9199
64. Song, Z. et al. *FIO-QLNM FIO-ESM2.0 Model Output Prepared for CMIP6 ScenarioMIP ssp585* Version 20210201 (Earth System Grid Federation, 2019); https://doi.org/10.22033/ESGF/CMIP6.9214
65. Guo, H. et al. *NOAA-GFDL GFDL-CM4 Model Output Prepared for CMIP6 CMIP Historical* Version 20210201 (Earth System Grid Federation, 2018); https://doi.org/10.22033/ESGF/CMIP6.8594
66. Guo, H. et al. *NOAA-GFDL GFDL-CM4 Model Output Prepared for CMIP6 ScenarioMIP ssp585* Version 20210201 (Earth System Grid Federation, 2018); https://doi.org/10.22033/ESGF/CMIP6.9268
67. Krasting, J. P. et al. *NOAA-GFDL GFDL-ESM4 Model Output Prepared for CMIP6 CMIP Historical* Version 20210201 (Earth System Grid Federation, 2018); https://doi.org/10.22033/ESGF/CMIP6.8597
68. Krasting, J. P. et al. *NOAA-GFDL GFDL-ESM4 Model Output Prepared for CMIP6 ScenarioMIP ssp585* Version 20210201 (Earth System Grid Federation, 2018); https://doi.org/10.22033/ESGF/CMIP6.8706

69. NASA Goddard Institute For Space Studies (NASA/GISS). *NASA-GISS GISS-E2.1G Model Output Prepared for CMIP6 CMIP Historical* Version 20210201 (Earth System Grid Federation, 2018); https://doi.org/10.22033/ESGF/CMIP6.7127
70. NASA Goddard Institute For Space Studies (NASA/GISS). *NASA-GISS GISS-E2.1G Model Output Prepared for CMIP6 ScenarioMIP ssp585* Version 20210201 (Earth System Grid Federation, 2020); https://doi.org/10.22033/ESGF/CMIP6.7460
71. Ridley, J. et al. *MOHC HadGEM3-GC31-LL Model Output Prepared for CMIP6 CMIP Historical* Version 20210201 (Earth System Grid Federation, 2019); https://doi.org/10.22033/ESGF/CMIP6.6109
72. Good, P. et al. *MOHC HadGEM3-GC31-LL Model Output Prepared for CMIP6 ScenarioMIP ssp585* Version 20210201 (Earth System Grid Federation, 2019); https://doi.org/10.22033/ESGF/CMIP6.10901
73. Ridley, J. et al. *MOHC HadGEM3-GC31-MM Model Output Prepared for CMIP6 CMIP Historical* Version 20210201 (Earth System Grid Federation, 2019); https://doi.org/10.22033/ESGF/CMIP6.6112
74. Jackson, L. *MOHC HadGEM3-GC31-MM Model Output Prepared for CMIP6 ScenarioMIP ssp585* Version 20210201 (Earth System Grid Federation, 2020); https://doi.org/10.22033/ESGF/CMIP6.10902
75. Volodin, E. et al. *INM INM-CM4-8 Model Output Prepared for CMIP6 CMIP Historical* Version 20210201 (Earth System Grid Federation, 2019); https://doi.org/10.22033/ESGF/CMIP6.5069
76. Volodin, E. et al. *INM INM-CM4-8 Model Output Prepared for CMIP6 ScenarioMIP ssp585* Version 20210201 (Earth System Grid Federation, 2019); https://doi.org/10.22033/ESGF/CMIP6.12337
77. Volodin, E. et al. *INM INM-CM5-0 Model Output Prepared for CMIP6 CMIP Historical* Version 20210201 (Earth System Grid Federation, 2019); https://doi.org/10.22033/ESGF/CMIP6.5070
78. Volodin, E. et al. *INM INM-CM5-0 Model Output Prepared for CMIP6 ScenarioMIP ssp585* Version 20210201 (Earth System Grid Federation, 2019); https://doi.org/10.22033/ESGF/CMIP6.12338
79. Boucher, O. et al. *IPSL IPSL-CM6A-LR Model Output Prepared for CMIP6 ScenarioMIP ssp585* Version 20210201 (Earth System Grid Federation, 2018); https://doi.org/10.22033/ESGF/CMIP6.5271
80. Byun, Y. H. et al. *NIMS-KMA KACE1.0-G Model Output Prepared for CMIP6 CMIP Historical* Version 20210201 (Earth System Grid Federation, 2019); https://doi.org/10.22033/ESGF/CMIP6.8378
81. Byun, Y. H. et al. *NIMS-KMA KACE1.0-G Model Output Prepared for CMIP6 ScenarioMIP ssp585* Version 20210201 (Earth System Grid Federation, 2019); https://doi.org/10.22033/ESGF/CMIP6.8456
82. Kim, Y. H. et al. *KIOST KIOST-ESM Model Output Prepared for CMIP6 CMIP Historical* Version 20210201 (Earth System Grid Federation, 2019); https://doi.org/10.22033/ESGF/CMIP6.5296
83. Kim, Y. H. et al. *KIOST KIOST-ESM Model Output Prepared for CMIP6 ScenarioMIP ssp585* Version 20210201 (Earth System Grid Federation, 2019); https://doi.org/10.22033/ESGF/CMIP6.11249
84. Stouffer, R. *UA MCM-UA-1-0 Model Output Prepared for CMIP6 CMIP Historical* Version 20210201 (Earth System Grid Federation, 2019); https://doi.org/10.22033/ESGF/CMIP6.8888
85. Stouffer, R. *UA MCM-UA-1-0 Model Output Prepared for CMIP6 ScenarioMIP ssp585* Version 20210201 (Earth System Grid Federation, 2019); https://doi.org/10.22033/ESGF/CMIP6.13901
86. Tachiiri K. et al. *MIROC MIROC-ES2L Model Output Prepared for CMIP6 ScenarioMIP ssp585* Version 20210201 (Earth System Grid Federation, 2019); https://doi.org/10.22033/ESGF/CMIP6.5770
87. Jungclaus, J. et al. *MPI-M MPI-ESM1.2-HR Model Output Prepared for CMIP6 CMIP Historical* Version 20210201 (Earth System Grid Federation, 2019); https://doi.org/10.22033/ESGF/CMIP6.6594
88. Steger, C. et al. *DWD MPI-ESM1.2-HR Model Output Prepared for CMIP6 ScenarioMIP ssp585* Version 20210201 (Earth System Grid Federation, 2019); https://doi.org/10.22033/ESGF/CMIP6.4479
89. Wieners, K.-H. et al. *MPI-M MPI-ESM1.2-LR Model Output Prepared for CMIP6 CMIP Historical* Version 20210201 (Earth System Grid Federation, 2019); https://doi.org/10.22033/ESGF/CMIP6.6595
90. Wieners, K.-H. et al. *MPI-M MPI-ESM1.2-LR Model Output Prepared for CMIP6 ScenarioMIP ssp585* Version 20210201 (Earth System Grid Federation, 2019); https://doi.org/10.22033/ESGF/CMIP6.6705
91. Yukimoto, S. et al. *MPI-M MPI-ESM1.2-LR Model Output Prepared for CMIP6 CMIP Historical* Version 20210201 (Earth System Grid Federation, 2019); https://doi.org/10.22033/ESGF/CMIP6.6842
92. Yukimoto, S. et al. *MRI MRI-ESM2.0 Model Output Prepared for CMIP6 ScenarioMIP ssp585* Version 20210201 (Earth System Grid Federation, 2019); https://doi.org/10.22033/ESGF/CMIP6.6929
93. Cao, J. & Wang, B. *NUIST NESMv3 Model Output Prepared for CMIP6 CMIP Historical* Version 20210201 (Earth System Grid Federation, 2019); https://doi.org/10.22033/ESGF/CMIP6.8769
94. Cao, J. *NUIST NESMv3 Model Output Prepared for CMIP6 ScenarioMIP ssp585* Version 20210201 (Earth System Grid Federation, 2019); https://doi.org/10.22033/ESGF/CMIP6.8790

95. Seland, Ø. et al. *NCC NorESM2-LM Model Output Prepared for CMIP6 CMIP Historical* Version 20210201 (Earth System Grid Federation, 2019); https://doi.org/10.22033/ESGF/CMIP6.8036
96. Seland, Ø. et al. *NCC NorESM2-LM Model Output Prepared for CMIP6 ScenarioMIP ssp585* Version 20210201 (Earth System Grid Federation, 2019); https://doi.org/10.22033/ESGF/CMIP6.8319
97. Bentsen, M. et al. *NCC NorESM2-MM Model Output Prepared for CMIP6 CMIP Historical* Version 20210201 (Earth System Grid Federation, 2019); https://doi.org/10.22033/ESGF/CMIP6.8040
98. Bentsen, M. et al. *NCC NorESM2-MM Model Output Prepared for CMIP6 ScenarioMIP ssp585* Version 20210201 (Earth System Grid Federation, 2019); https://doi.org/10.22033/ESGF/CMIP6.8321
99. Tang, Y. et al. *MOHC UKESM1.0-LL Model Output Prepared for CMIP6 CMIP Historical* Version 20210201 (Earth System Grid Federation, 2019); https://doi.org/10.22033/ESGF/CMIP6.6113
100. Good, P. et al. *MOHC UKESM1.0-LL Model Output Prepared for CMIP6 ScenarioMIP ssp585* Version 20210201 (Earth System Grid Federation, 2019); https://doi.org/10.22033/ESGF/CMIP6.6405